

## Selective Isomerization of $\alpha$ -pinene oxide to Trans-Carveol by Task-Specific Ionic Liquids: Mechanistic insights via Physicochemical studies

Sanjay Mehra<sup>a,c#</sup> Dhanaji R. Naikwadi<sup>b,c#</sup> Kuldeep Singh<sup>a,c</sup> Ankush V. Biradar<sup>b,c\*</sup> and Arvind Kumar<sup>a, c\*</sup>

<sup>a</sup>Salt and Marine chemicals Division, CSIR-Central Salt & Marine Chemicals Research Institute, G. B. Marg, Bhavnagar-364002, Gujarat, India

<sup>b</sup>Inorganic Materials and Catalysis Division, CSIR-Central Salt & Marine Chemicals Research Institute, G. B. Marg, Bhavnagar-364002, Gujarat, India

<sup>c</sup>Academy of Scientific and Innovative Research (AcSIR), Ghaziabad-201002, India

#The Authors are contributed equally

\*Corresponding author: E-mail: [ankush@csmcri.res.in](mailto:ankush@csmcri.res.in), [arvind@csmcri.res.in](mailto:arvind@csmcri.res.in)

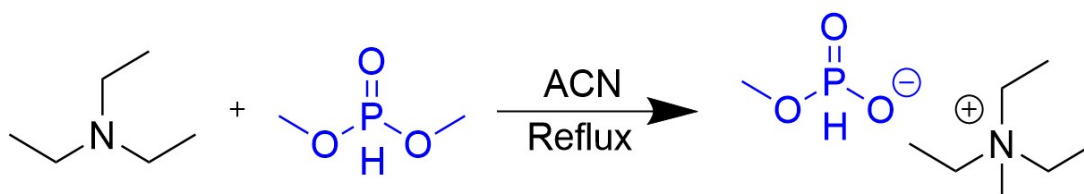
Entry	Content	Page No
1	General information	S1-S2
2	Characterizations of synthesized ILs	S3-S6
3	Thermodynamic parameters investigation of synthesized ILs	S6-S9
4	Polarizability/ dipolarity of synthesized ILs	S9-S11
5	Organic transformation of pinene oxide using ILs and recycle studies	S11-S13
6	Green metrics	S13-S14
7	References	S15

### Materials

Pyridine with purity  $\geq 99.0$ , 3, 5 Lutidine with purity  $\geq 98\%$ , and Dimethyl phosphite with a purity of 98% were purchased from Sigma Aldrich. Triethylamine with purity  $\geq 99.5$ , Ethylacetate, Acetonitrile and methanol with AR grade were purchased from Lobachemei.  $\alpha$ -pinene oxide from TCI india.

### Synthesis of ILs-

a) **Triethylmethylammonium methyl phosphonate** - A slightly modified procedure was followed to synthesize triethylmethylammonium methyl phosphonate TEMA[MeOPHO<sub>2</sub>] IL.<sup>1</sup> A 500 mL three-necked round-bottomed flask was equipped with a reflux condenser with a drying tube containing calcium chloride, a gas inlet adapter and an addition funnel with a pressure equalizer arm was flushed with nitrogen and filled with 250 mL acetonitrile. After that, 11.0 g of dimethyl phosphite (0.1 mol) and 10.0 g (0.0988 mol) of triethylamine were added dropwise under vigorous stirring and refluxed for 24 h under a nitrogen environment. After the completion of the reaction solvent was removed using a rotary evaporator at 70 °C by reducing the pressure and obtained product was washed with excess diethyl ether/ ethyl acetate. Again traces of washing solvents were evaporated using a rotary evaporator and later put under a high vacuum to remove high boiling point impurities. In the end, the transparent liquid was obtained, which was transferred to air-tight bottles and stored in a desiccator under low pressure. The synthesis of ILs was shown in Scheme 1.



Scheme-S1. Synthetic procedure for ILs

b) **3,5 Lutidinium methyl phosphonate** - Above mentioned procedure was followed to synthesize 3,5 lutidinium methyl phosphite Lut[MeOPHO<sub>2</sub>] in which 11.0 g of dimethyl phosphite (0.1 mol) and 10.58 g (0.0988 mol) of 3,5-Lutidine were added dropwise under vigorous stirring and refluxed for 24 h under a nitrogen environment. After completion of the reaction, the process described (TEMA[MeOPHO<sub>2</sub>] synthesis Section) above was used to purify the IL.

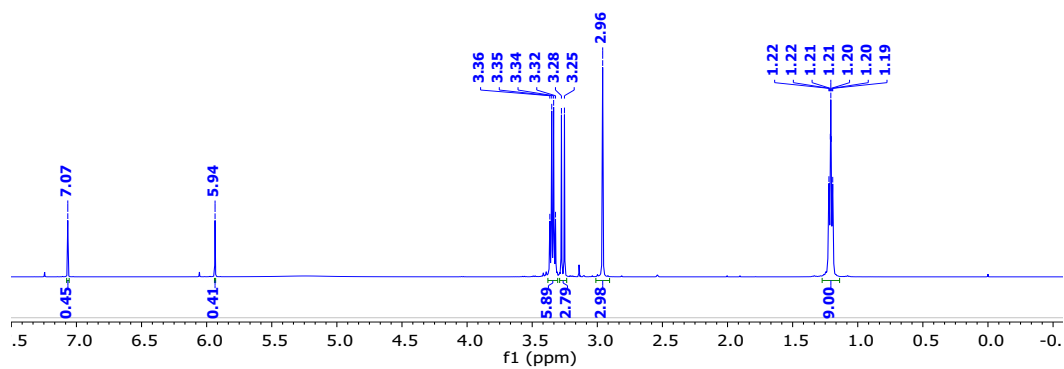
c) **Pyridinium methyl phosphonate** - Above mentioned procedure was followed to synthesize pyridinium methyl phosphite Py[MeOPHO<sub>2</sub>] in which 11.0 g of dimethyl phosphite (0.1 mol) and 7.81 g (0.0988 mol) of pyridine was added dropwise under vigorous stirring and refluxed for 24 h under a nitrogen environment. After completion of the reaction, the process described (TEMA[MeOPHO<sub>2</sub>] synthesis Section) above was used to purify the IL. The purity of all synthesized ILs was characterized using <sup>1</sup>H, <sup>13</sup>C and <sup>31</sup>P NMR.

### **Physicochemical characterizations**

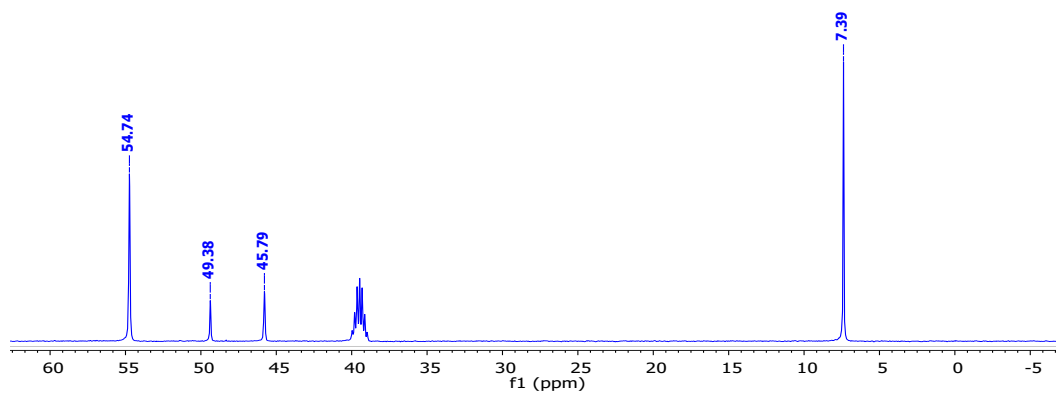
All ILs were dried in a vacuum for 12 hours and handled carefully to minimize the moisture content. UV–vis absorption spectrums were recorded using a Varian Cary 500 UV-Vis NIR spectrophotometer. Phase transition points ( $T_g$ ), crystallization temperatures ( $T_c$ ), and melting points ( $T_m$ ) were measured on a DSC NETZCH DSC 204 F<sub>1</sub> Phoenix thermal analyzer at the scan rate of 10 K min<sup>-1</sup>. Decomposition temperatures ( $T_d$ ) measurements were performed on a NETZSCH TG 209 F<sub>1</sub> Libra thermogravimeter under N<sub>2</sub> atmosphere at a heating rate of 10 K min<sup>-1</sup> in the temperature range of 303.15 to 1073.15 K. Densities ( $\rho$ ) and sound velocities ( $u$ ) measurements from 293.15 K to 343.15 K in 5 K steps were carried out using an Anton Paar Model DSA 5000 with a vibrating tube density meter with a resolution of  $5 \times 10^{-6}$  g.cm<sup>-3</sup> and 0.01m.s<sup>-1</sup> for the density and speed of sound respectively. Dynamic viscosity ( $\eta$ ) measurements from 293.15 K to 343.15 K in 5 K steps were carried out using an AMVn Automated Micro Viscometer (Anton Paar, Graz, Austria) with a ball rolling capillary method.

# 1. Characterizations of synthesized ILs

(a)



(b)



(c)

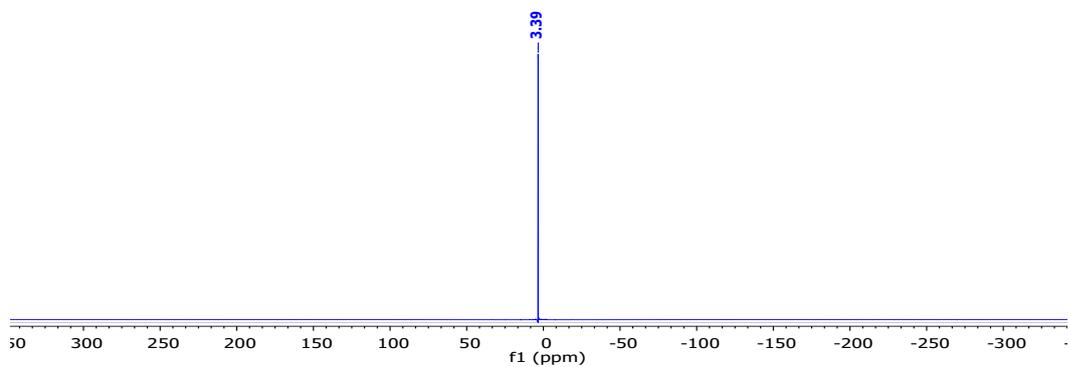


Figure S1. (a) <sup>1</sup>H, (b) <sup>13</sup>C and (c) <sup>31</sup>P NMR spectrums of TEMA[MeOPHO<sub>2</sub>]

## a. NMR analysis

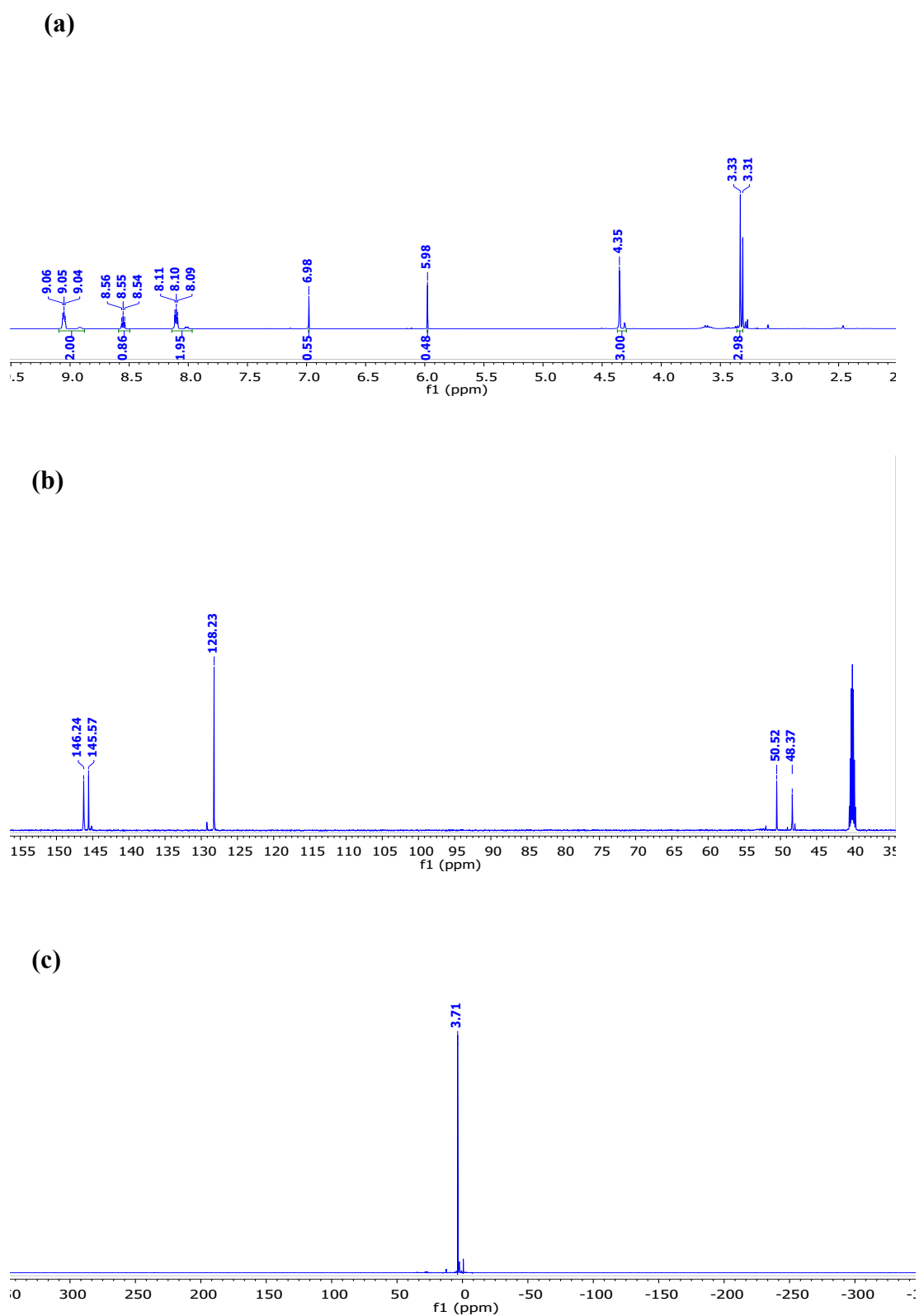


Figure S2. (a) <sup>1</sup>H, (b) <sup>13</sup>C and (c) <sup>31</sup>P NMR spectra of Py[MeOPHO<sub>2</sub>]

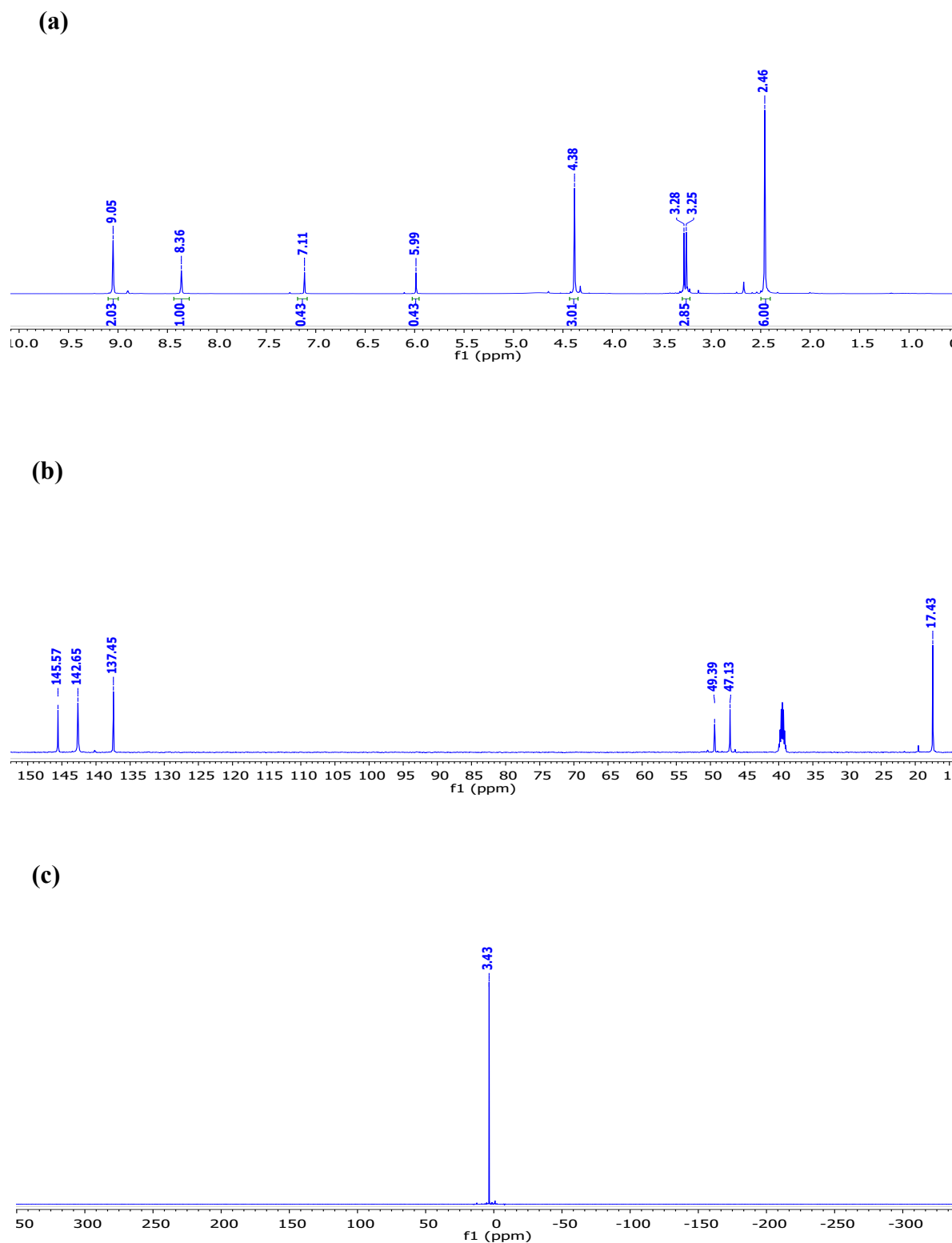


Figure S3. (a) <sup>1</sup>H, (b) <sup>13</sup>C and (c) <sup>31</sup>P NMR spectra of Lut[MeOPHO<sub>2</sub>]

*DSC and TGA analysis*

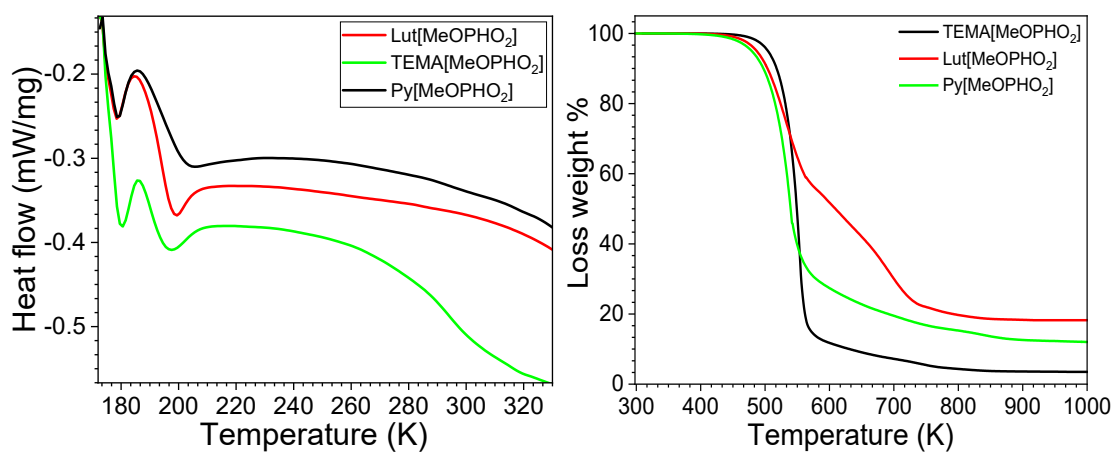


Figure S4. (a) DSC and (b) TGA thermograms of synthesized ILs

## 2. Characterizations of isolated product

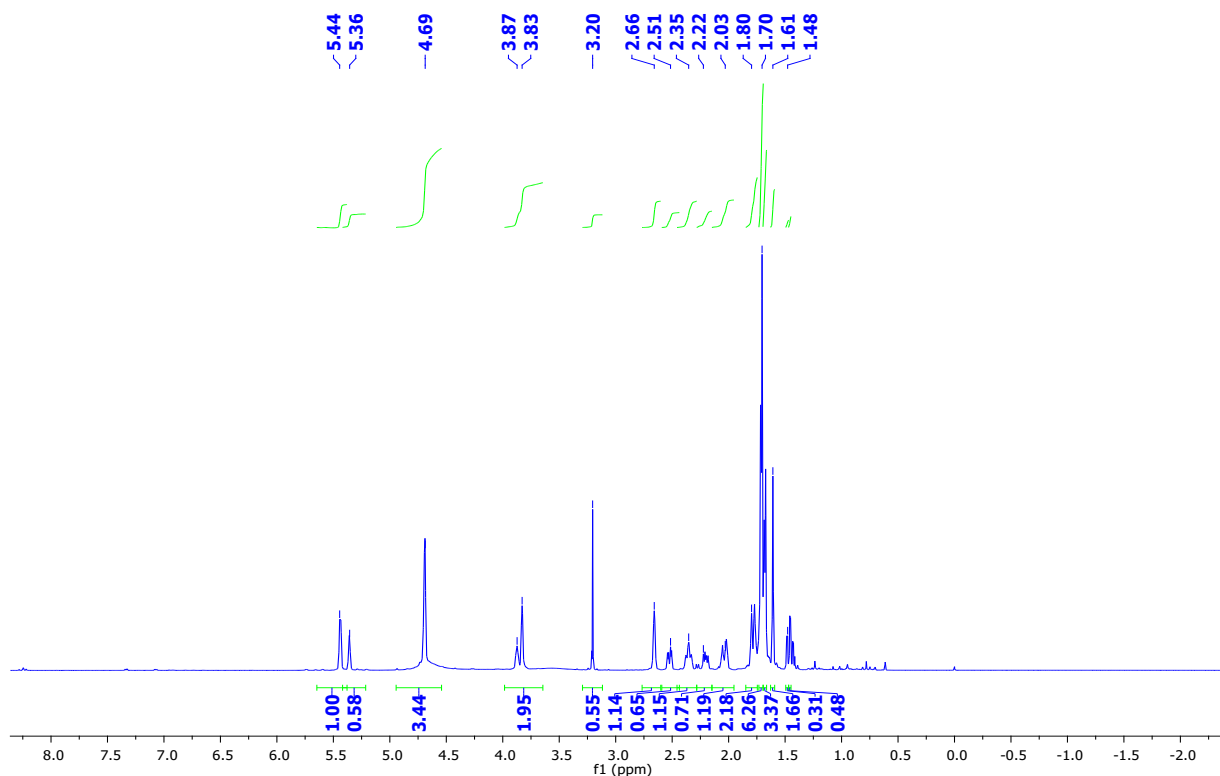


Figure S5. <sup>1</sup>H-NMR of Trans-carveol

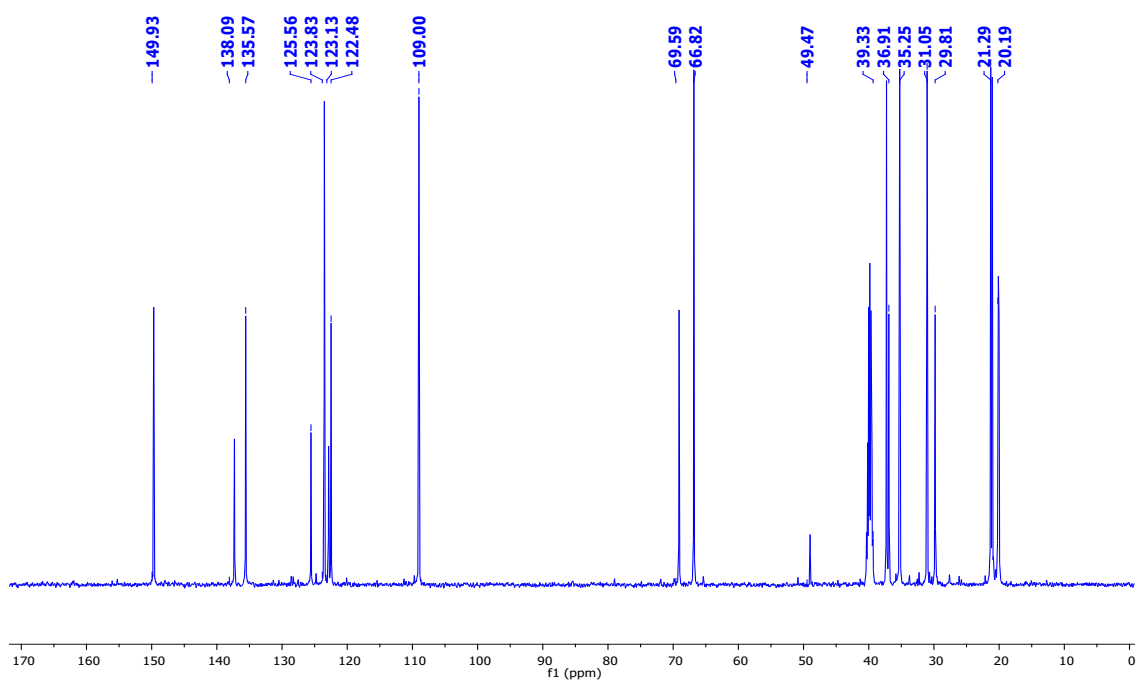


Figure S6.  $^{13}\text{C}$ -NMR of Trans-carveol

Line#:1 R.Time:10.575(Scan#:1496)  
 MassPeaks:309  
 RawMode:Averaged 10.570-10.580(1495-1497) BasePeak:109(72340)  
 BG Mode:Calc. from Peak Group 1 - Event 1

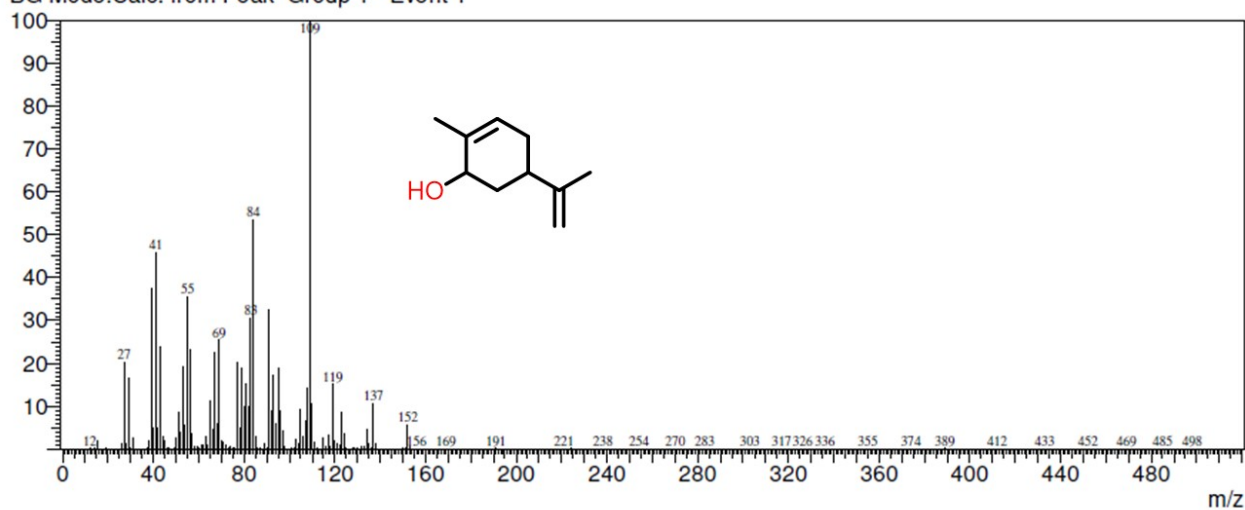


Figure S7. GSMS chromatogram of Trans-carveol

Line#:1 R.Time:9.505(Scan#:1282)  
MassPeaks:310  
RawMode:Averaged 9.500-9.510(1281-1283) BasePeak:108(1721715)  
BG Mode:Calc. from Peak Group 1 - Event 1

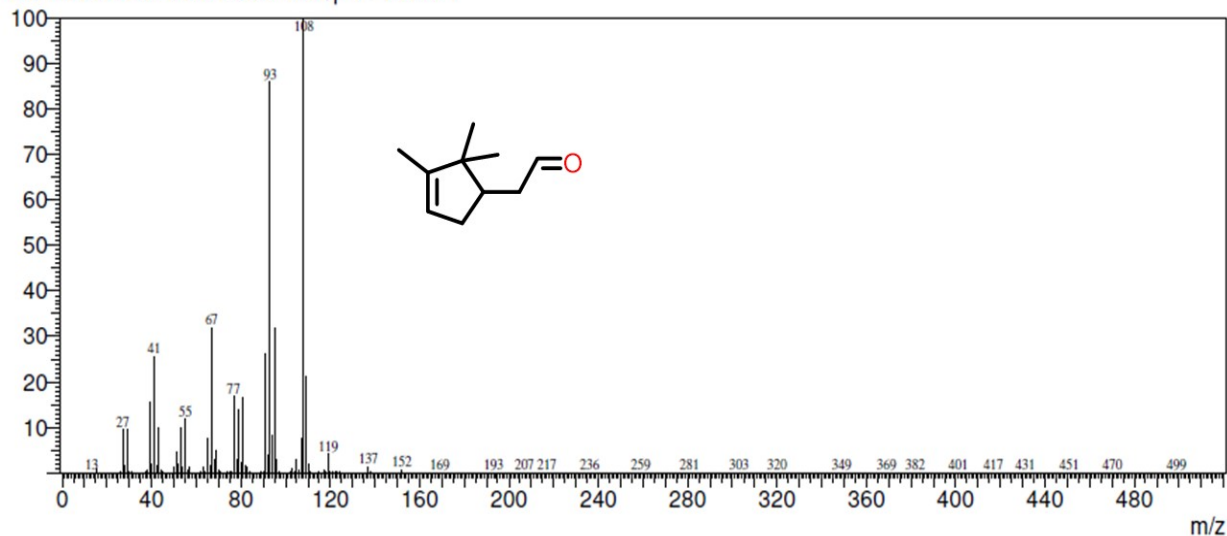


Figure S8. GSMS chromatogram of Alpha Campholenic Aldehyde

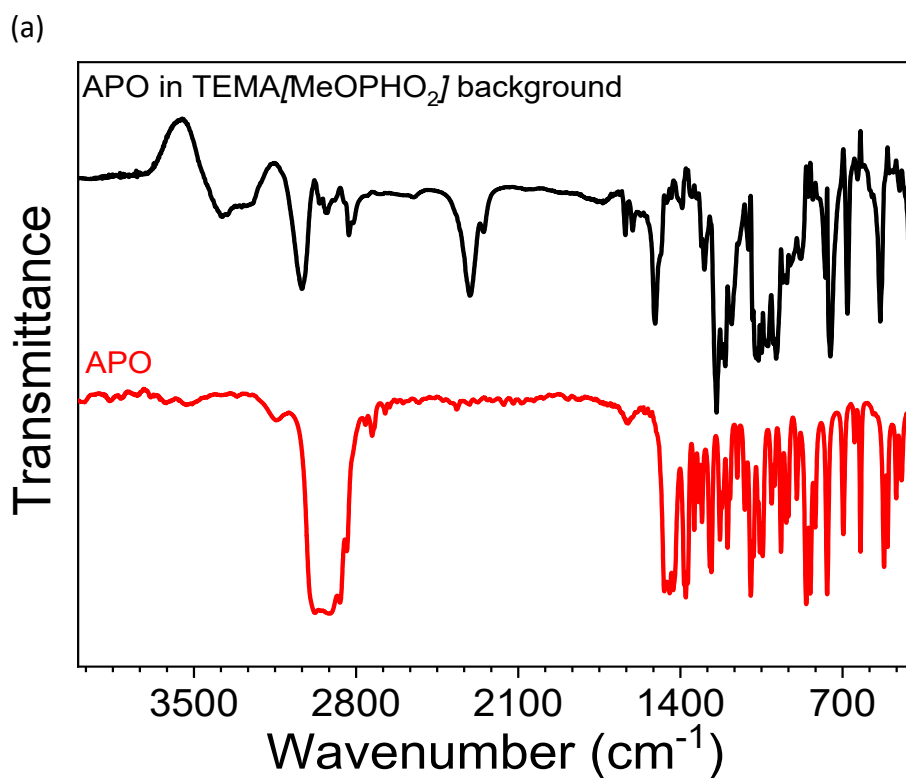
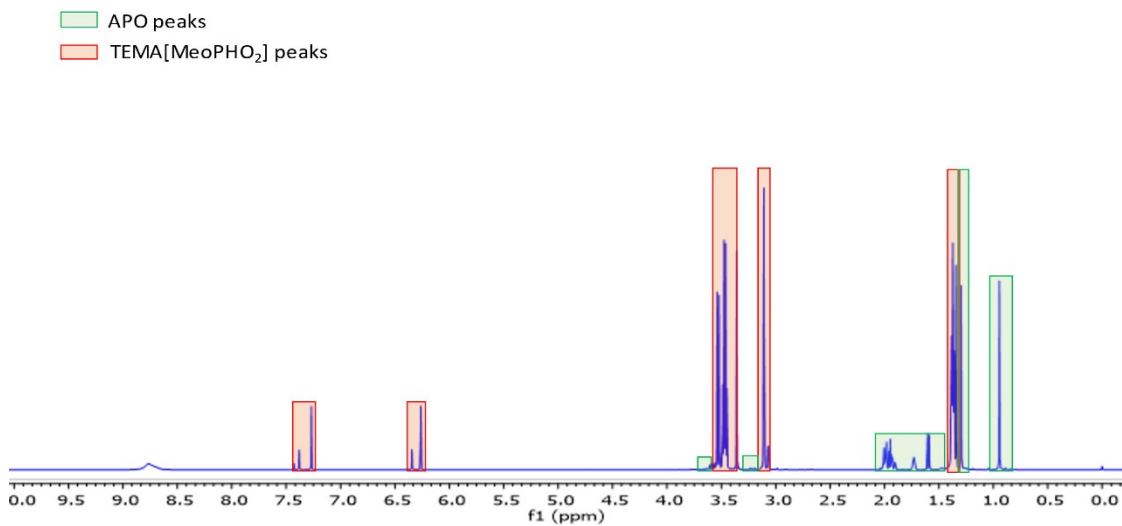
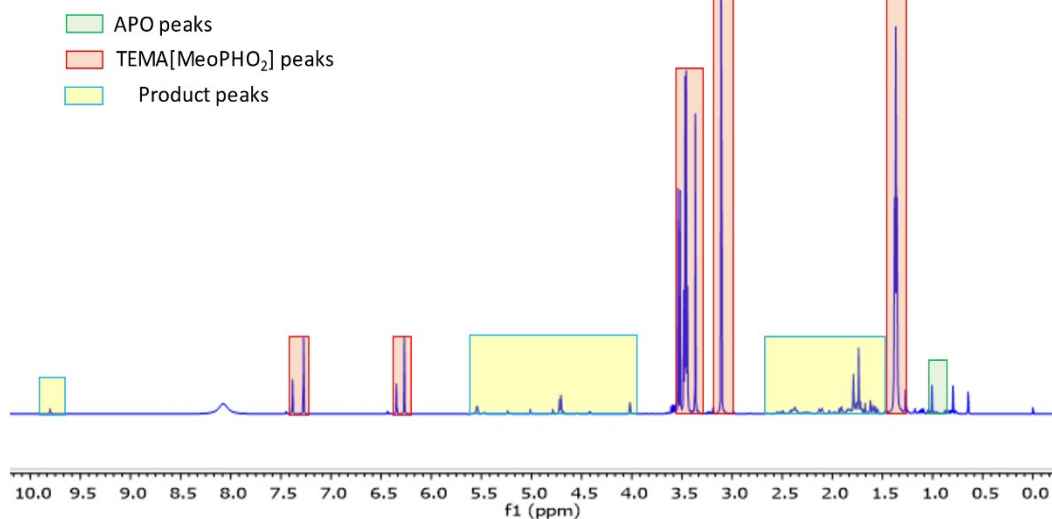


Figure S9. Mechanistic studies by FTIR of APO and APO with IL background

(a)



(b)



(c)

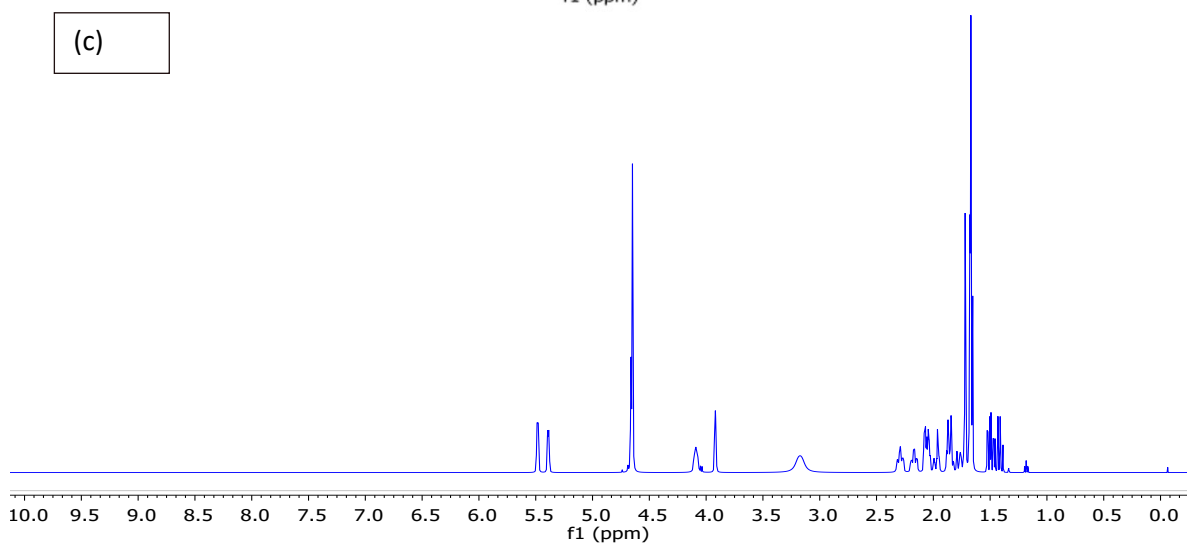


Figure S10. Mechanistic studies by <sup>1</sup>H NMR (a) APO + TEMA[MeOPHO<sub>2</sub>], (b) APO + TEMA[MeOPHO<sub>2</sub>] after 3 h heated at 413.15 K (c) Isolated TCV

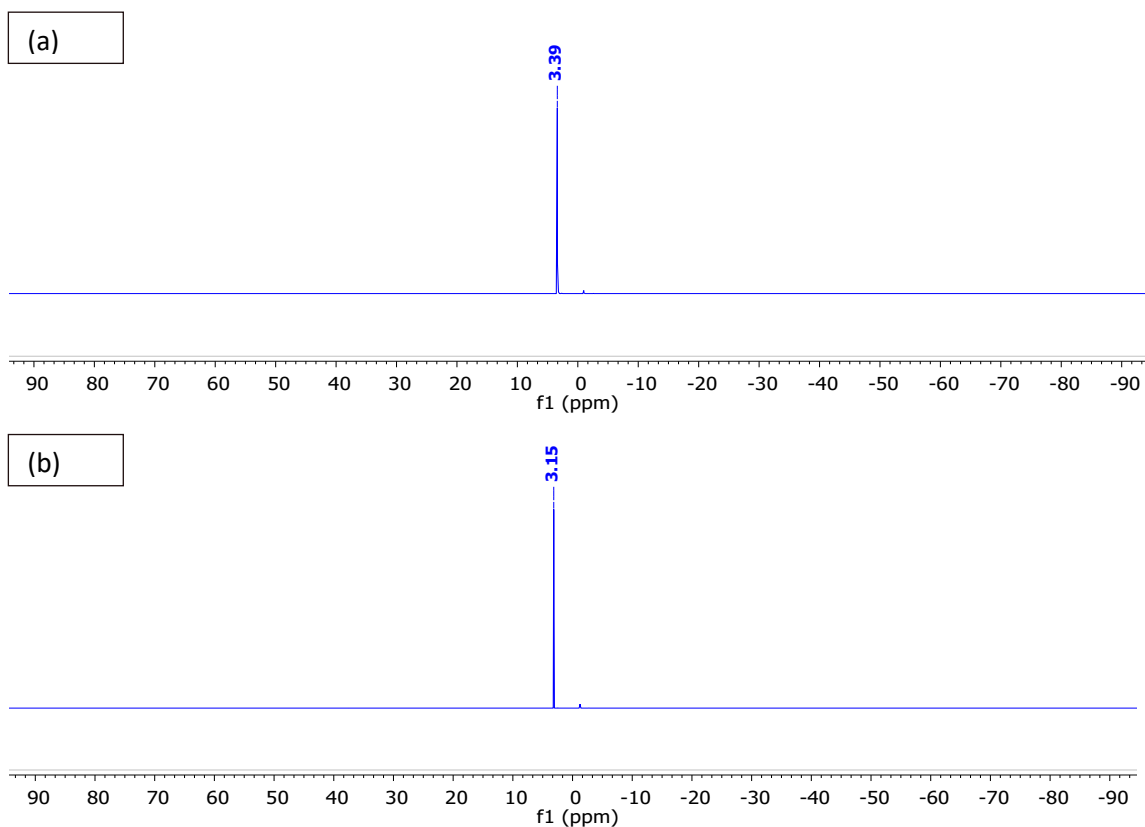


Figure S11. Mechanistic studies by  $^{31}\text{P}$  NMR (a) TEMA[MeOPHO<sub>2</sub>], (b) APO + TEMA[MeOPHO<sub>2</sub>].

### 3. Thermodynamic parameters investigation of synthesized ILs

#### (a) Conductivity ( $\kappa$ ) and Walden rule

The classical Walden rule is usually used for assessing the ionicity of ILs. The ionic mobilities (represented by the equivalent conductivity  $\Lambda = F \sum \mu_i Z_i$ ) and the fluidity  $\varphi$  ( $\varphi = \eta^{-1}$ ) of the medium can be related to the Walden rule by the movement of the ions. The relationship between the  $\Lambda$  and  $\eta$  of ILs can be described as:

$$\Lambda \eta = k \quad (\text{S1})$$

Where  $\Lambda$  is the molar electrical conductivity,  $\eta$  is the dynamic viscosity, and  $k$  is a temperature-

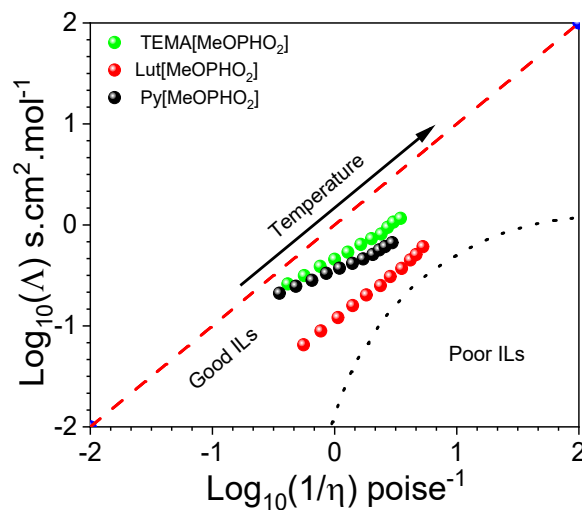


Figure S12. Walden plot of synthesized ILs with temperature.

dependent constant.

**(b) Dynamic viscosity**

The thermodynamic flow activation parameters Gibbs energy of activation ( $^\ddagger\Delta G$ ), enthalpy of activation ( $^\ddagger\Delta H$ ), the entropy of activation ( $^\ddagger\Delta S$ ) and variation of the calorific capacity of activation ( $^\ddagger\Delta C_p$ ) were estimated from the Eyring equation.<sup>2</sup>

$$\eta = \frac{hN_a}{V_M} \exp\left(\frac{^\ddagger\Delta G}{RT}\right) \quad (\text{S2})$$

where  $\eta$  is the dynamic viscosity,  $h$  is the Planck constant,  $N_a$  is the Avogadro constant,  $V_M$  is the molecular volume,  $R$  is the universal gas constant, and  $T$  is the absolute temperature.

According to the thermodynamic law  $^\ddagger\Delta G$ ,

$$^\ddagger\Delta G = ^\ddagger\Delta H - T^\ddagger\Delta S \quad (\text{S3})$$

The  $V_M$ ,  $\Delta H$ , and  $\Delta S$  are considered temperature-dependent herein. Thus, the constraints can be applied in broader ranges of temperature.  $^\ddagger\Delta G$  is calculated by isolating it from the Eyring equation.  $^\ddagger\Delta H$  is obtained by using the Gibbs-Helmholtz equation.

$$^\ddagger\Delta H = \left( \frac{\partial(^\ddagger\Delta G/T)}{\partial(1/T)} \right) \quad (S4)$$

Thus,  $^\ddagger\Delta H$  is calculated by the derivation of function  $^\ddagger\Delta G/T$  with respect to  $1/T$ .  $^\ddagger\Delta C_p$  is given by the derivation of the activation enthalpy  $^\ddagger\Delta H$  to temperature.  $^\ddagger\Delta S$  is calculated from its

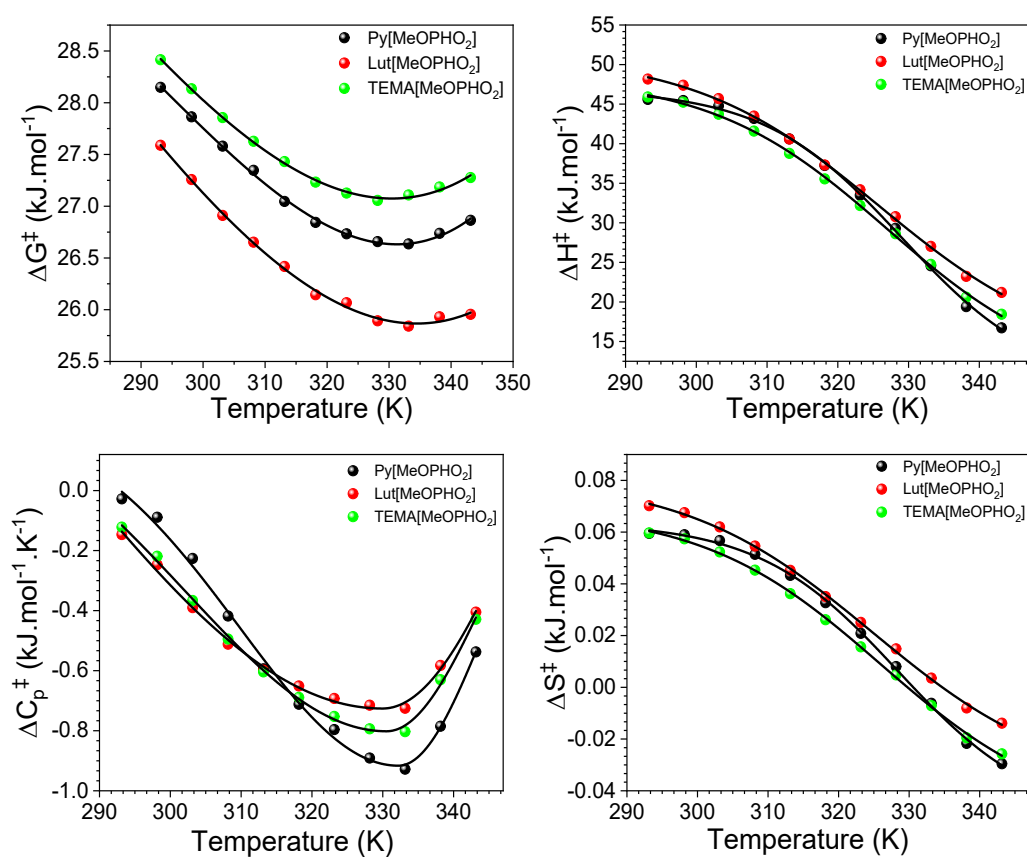


Figure S13. (a) Gibbs energy of activation, (b) enthalpy of activation, (c) standard molar entropy and (d) variation of calorific capacity of activation of synthesized ILs with temperature.

thermodynamic equation (Equation S2).  $\eta$  may be described by any previously mentioned empirical models for viscosity.

**(c) Density**

The investigation of the volumetric properties of ILs was done as per the literature. A straight line can be obtained according to plot  $\ln\rho$  against  $T/K$ . The  $\ln\rho$  against  $T/K$  can be fitted by the following empirical equation:

$$\ln\rho = b - \alpha T \quad (S5)$$

Where  $b$  is an empirical constant and  $\alpha$  is the thermal expansion coefficient.

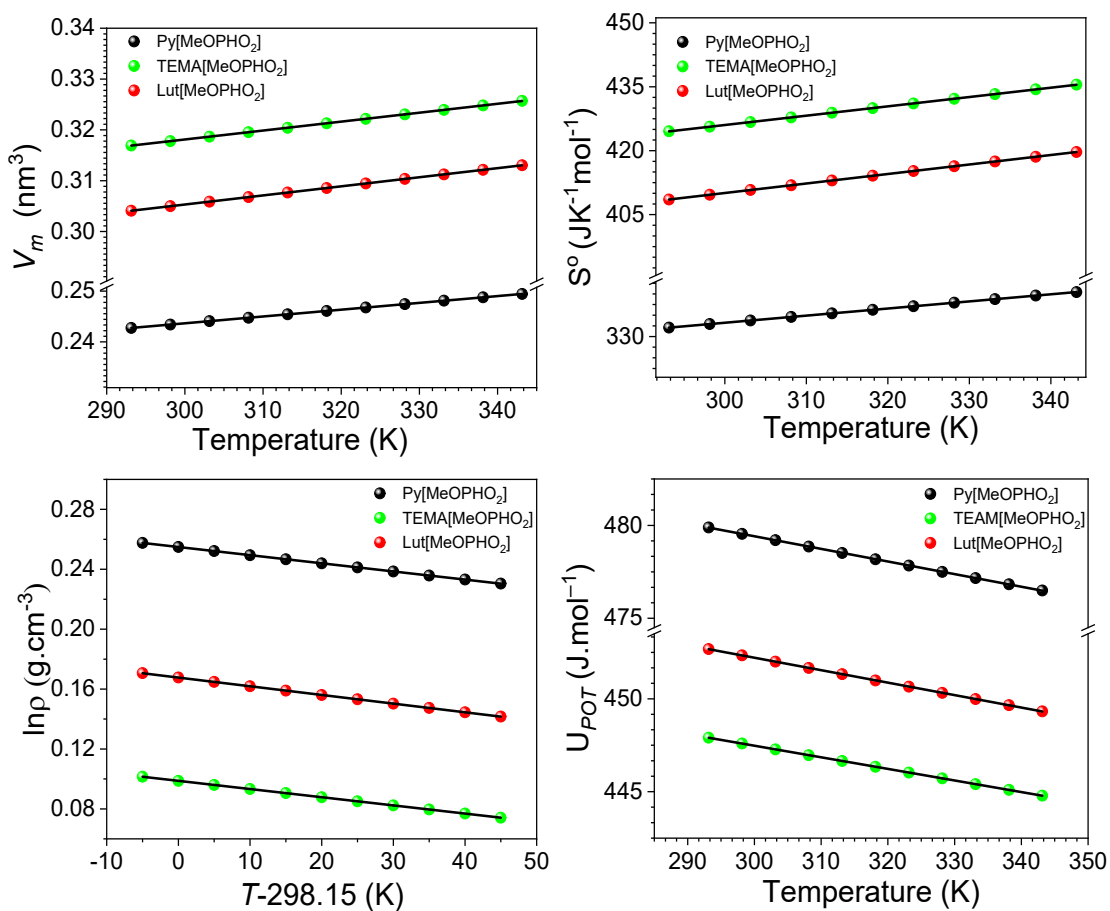


Figure S14. (a) Molecular volume, (b) standard molar entropy, (c) thermal expansion coefficient and (d) lattice energy.

At 298.15 K, the molecular volume,  $V_m$ , standard molar entropy,  $S^0$ , and lattice energy,  $U_{POT}$ , of the ILs can be obtained from the experimental density by the following equations:

$$V_m = \frac{M}{\rho N_a} \quad (S6)$$

$$S^0 = 1246.5 \cdot (V_m) + 29.5 \quad (S7)$$

$$U_{POT} = 1981.2 \cdot \left(\frac{\rho}{M}\right)^{\frac{1}{3}} + 103.8 \quad (S8)$$

where,  $M$  is molar mass,  $\rho$  is the density, and  $N_a$  is Avogadro's constant.

#### 4. Polarizability/ dipolarity of synthesized ILs

##### *Kamlet taft parameters*

The negative solvatochromism of Reichardt's dye has been widely used to investigate the polarity of ILs. Reichardt's dye has a significant permanent dipole moment for dipole-dipole or dipole-induced dipole interactions, an effective polarizable arrangement for dispersion interactions with a high electron-pair donor for hydrogen bonding interactions. The significant negative solvatochromism of dye is due to different dipolar excited states of the molecule. When IL polarity increases, the molecule's ground state is stabilized in solvation relative to the excited state. IL polarity parameters,  $E_T^N$ , is determined by intermolecular charge-transfer absorption of the dye in an IL. The normalized  $E_T^N$  represents a solvent polarity normalized using water and tetramethyl silane. 4-nitroaniline and N, N-diethyl-4-nitroaniline are commonly used to evaluate these parameters by solvatochromic comparisons of UV-spectra. This indicates the hydrogen-bond-donor acidity ( $\alpha$ ), hydrogen-bond-acceptor basicity ( $\beta$ ), and polarizability of ILs.

##### (1) Solvent Polarizability ( $\pi^*$ )

$$\pi^* = \frac{\nu(DENA)_{\max} - 27.52}{-3.183} \quad (S9)$$

where,

$$\nu(DENA)_{\max} = \frac{10000}{\lambda_{\max}(DENA)}$$

##### (2) Hydrogen Bond Donator Capacity ( $\alpha$ )

$$\alpha = \frac{E_T(30) - 14.6(\pi^* - 0.23) - 30.31}{16.5} \quad (\text{S10})$$

where,

$$E_T(30) = \frac{28591}{\lambda_{\max}(RD)}$$

(3) Hydrogen Bond Acceptor Capacity ( $\beta$ )

$$\beta = \frac{1.035 \times \nu_{\max}(DNA) - \nu_{\max}(4NA) + 2.64}{2.8} \quad (\text{S11})$$

where,

$$\nu_{\max}(4NA) = \frac{10000}{\lambda_{\max}(4NA)}$$

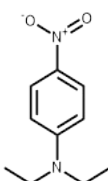
(4)

$$E_N^T = \frac{E_T(30) - 30.7}{32.7} \quad (\text{S12})$$

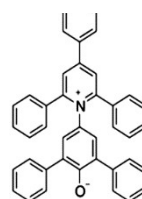
RD = Reichardt's dye

DENA= N,N-diethyl-4-nitroaniline

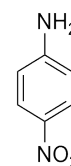
NA= 4-Nitroaniline



N,N diethyl  
4-nitroaniline



Reichardt's Dye



4-Nitroaniline

**Table S1:** Catalytic performance of recycled TEMA[MeOPHO<sub>2</sub>] TSIL

Entry	Recycle	Conversion%	Selectivity%		
			CV	CA	Others
1.	Fresh	99	74	26	-
2.	1	99	73	27	-
3.	2	99	75	25	-
4.	3	98	74	26	-
5.	4	98	74	26	-
6.	5	97	73	23	4

**Reaction conditions:** 0.5 mL APO, 413.15 K, 1.5 mL ILs, 3 h.

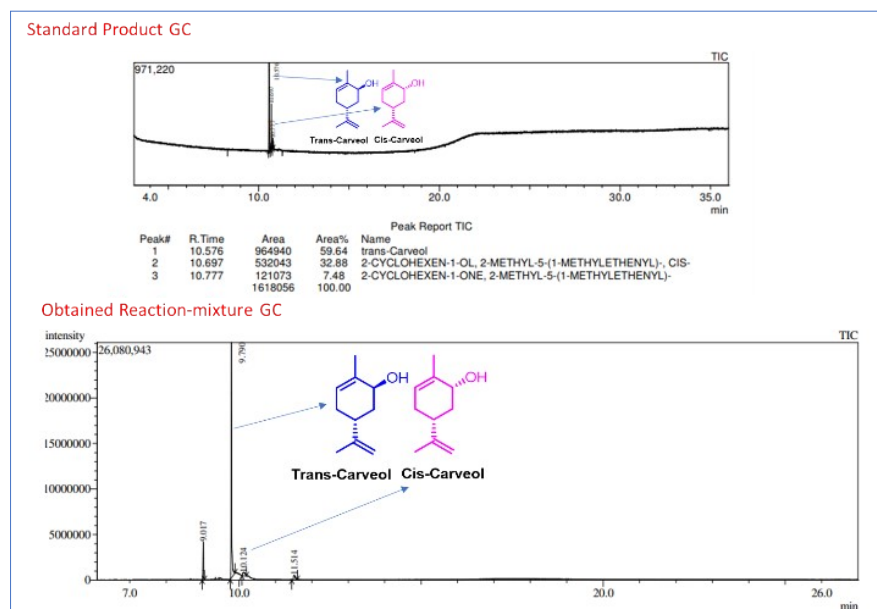


Figure S15. Show GC standard data of TCV and obtained reaction mixture.

**5. Recyclability of TEMA[MeOPHO<sub>2</sub>] IL** – When the reaction was finished, a biphasic system was created by mixing water and ethyl acetate in a separating funnel. TEMA[MeOPHO<sub>2</sub>] was isolated in the aqueous phase, while the products TCV and CA were isolated in the ethyl acetate phase. To eliminate minute organic contaminants, the recovered aqueous phase underwent one more ethyl acetate wash. To get regenerated TEMA[MeOPHO<sub>2</sub>] IL, rotary evaporation of the aqueous phase is performed. <sup>1</sup>H NMR was used to assess the purity of recycled IL.



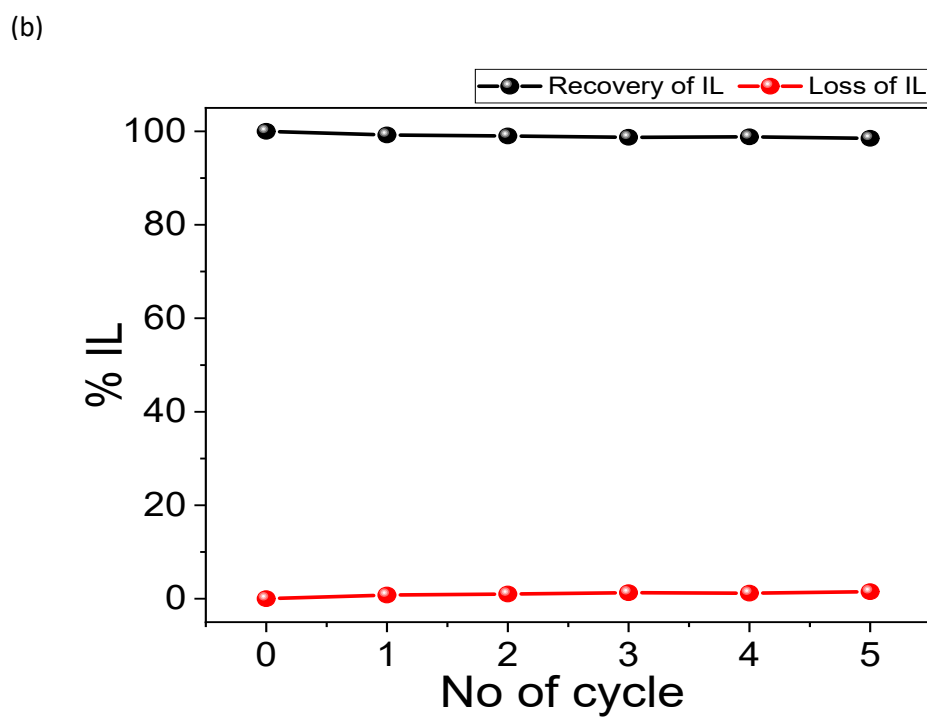
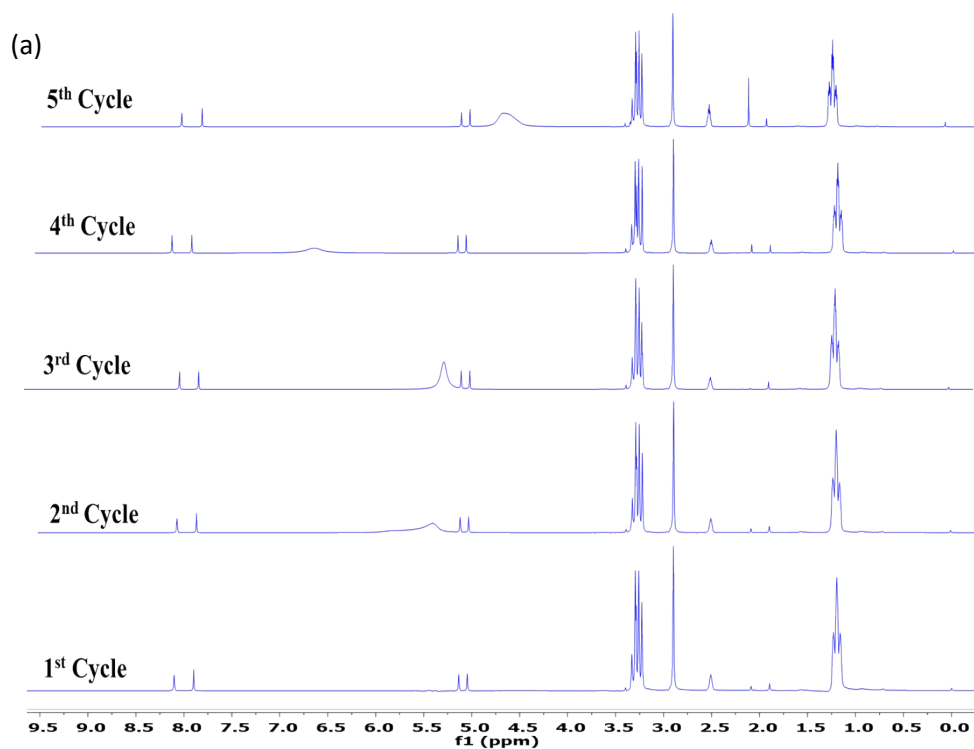
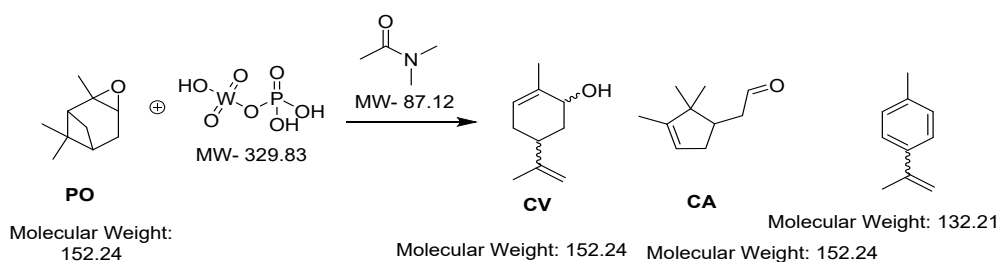
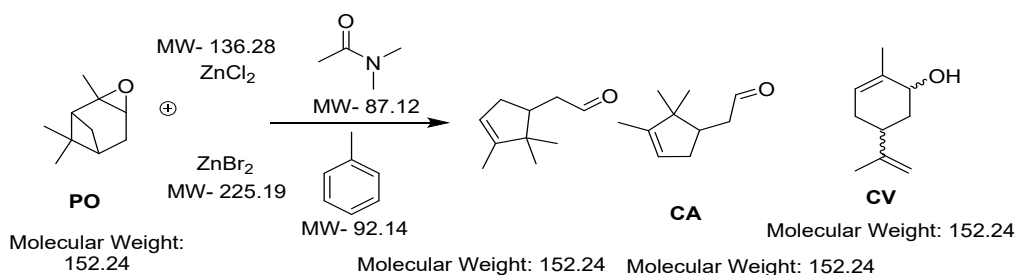


Figure S16. (a)  $^1\text{H}$  NMR (b) % of recovery of recycled TEMA[MeOPHO<sub>2</sub>] IL up to five cycles

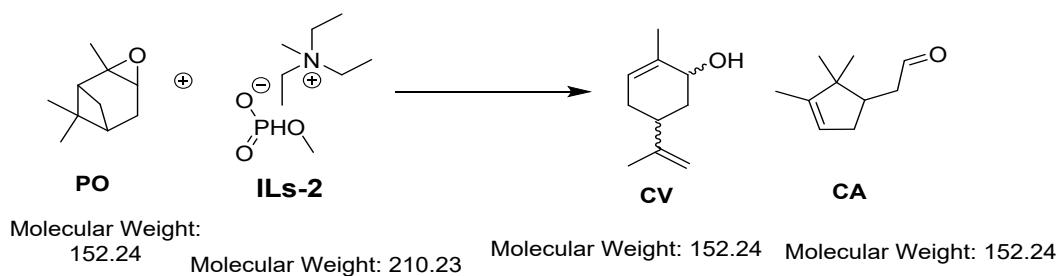
## 6. Green metrics for organic transformation



### Scheme S2a. Phosphotungstic acid-catalyzed isomerization of PO



### Scheme S2b. Zinc-catalyzed isomerization of PO into CV and CA



### Scheme S2c. Present work ILs catalyzed isomerization of PO

**Table S2.** The calculated green metrics for compounds (Comparison between literature and current work)

Entry	Comp No.	AE (%)	E (%)	MI (%)	MP (%)	EMY (%)	SI (%)	Ref.
1	A	100	1.86	3.73	26.74	1.74	0.57	3, 4
2	B	100	2	3.97	25.12	No hazardous reactant	0.60	
3	Current work	100	1.0	2.38	42.00	No hazardous reactant	0.0	

**Table 3. The calculated green metrics for ILs synthesis**

Entr	ILs scheme	AE (%)	E (%)	MI (%)	MP (%)	EMY (%)	Sel. (%)	Ref.
1	A	99.91	1.0	1.0	83.73	0.00	Cis-trans = 97-2.9	5
2	D-Limonene( <i>R. globerulus</i> PWD8.), 15-40°C 24 h.						Trans-74	6
3	(+)-Limonene/ (-)-limonene, ethanol, room temperature, 2h.							7
4							40	8
5	Limonene, 25°C, 6h.			immobilized cyanobacterial			24% Cis-	9
6	APO			( <i>Synechococcus</i> sp. PCC)			31-9	
6	APO			Molecularly Imprinted Polymers (MIPs)	100		Trans-45	10
7	APO in DMF, 120°C, 3h.			H <sub>3</sub> PW <sub>12</sub> O <sub>40</sub>	94		Trans-93	11
8	APO in DMA, 140°C, 8h.			Ce/SiO <sub>2</sub> and Sn/SiO <sub>2</sub>	98		Trans-73	12
9	APO in DMA, 140°C, 3h.			Ce-Si-MCM-41	100		Trans-41%	13
10	APO in DMA, 140°C, 3h.			Fe- Beta-300	100		Trans-43%	14
11	Limonene			Hydrogen peroxide and t-butyl hydroperoxide	-		74	15

10 g triethylamine (MW 101.19 g/mol) + 11 g dimethylphosphite (110.049 g/mol) in 250 ml Acetonitrile (MW 41.05 g/mol)  
 MW of ILs = 211.23 g/mol

12	D-limonene	<i>Pseudomonas putida</i> S12	-	Trans-carveol	16
13,	APO in DMF, 160°C. 1.5 h	N-C-SO <sub>3</sub> H	100	Trans-85%	17
14	APO in DMF, 140°C 1h	PCS ( $\alpha$ 2)	100	Trans-67%	18
15	APO in DMSO, 70°C 3h	20Mo450	45	Trans-53%	19
16	APO in THF, RT, 1h	Formic acid	100	Trans-62%	20
17	APO in DMA, 160°C, 5 h	ZrP <sub>3</sub>	100	Trans-76%	21
18	APO in DMA, 140°C. 3h	MZ-4 and MZ-5	70	Trans-44%	22
<b>19</b>	<b>APO in ILs, 140°C. 3h</b>	-	<b>99</b>	<b>74</b>	<b>Present work</b>

## References

1. D. R. Naikwadi, S. Mehra, K. Ravi, A. Kumar and A. V. Biradar, *ACS Sustainable Chemistry & Engineering*, 2022, **10**, 8526-8538.
2. L. J. dos Santos, L. A. Espinoza-Velasquez, J. A. P. Coutinho and S. Monteiro, *Fluid Phase Equilib.*, 2020, **522**, 112774.
3. J. Kaminska, M. A. Schwegler, A. J. Hoefnagel and H. van Bekkum, *Recl. Trav. Chim. Pays-Bas*, 1992, **111**, 432-437.
4. K. A. da Silva Rocha, J. L. Hoehne and E. V. Gusevskaya, *Chemistry*, 2008, **14**, 6166-6172.
5. Dictionary of organic compounds; 5th ed. Buckingham, J. Ed. Chapman and Hall: London, 1982; p I-01178.
6. W. Duetz, B. Witholt, and C. Jourdat, Eidgenoessische Technische Hochschule Zurich ETHZ, 2005. U.S. Patent Application 10/416,125.US20050260725A1.
7. M. Miyazawa, M. Shindo, and T. Shimada, *Chem. Res. Toxicol.* 2002, **15**, 15-20
8. H. Hamada, Y. Kondo, K. Ishihara, N. Nakajima, H. Hamada, R. Kurihara and T. Hirata, *J. Biosci. Bioeng.*, 2003, **96**, 581-584.
9. J. Kaminska, M. A. Schwegler, A. J. Hoefnagel and H. van Bekkum, *Recl. Trav. Chim. Pays-Bas* 1992, **111**, 432-437.
10. W. B. Motherwell, M. J. Bingham, J. Pothier and Y. Six, *Tetrahedron*, 2004, **60**, 3231-3241.
11. K. A. da Silva Rocha, J. L. Hoehne and E. V. Gusevskaya, *Chem. – Eur. J.*, 2008, **14**, 6166 –6172.
12. V. V. Costa, K. A. da Silva Rocha, L. F. de Sousa, P. A. Robles-Dutenhefner and E. V. Gusevskaya, *J. Mol. Catal. A: Chem.*, 2011, **345**, 69-74.

13. M. Stekrova, N. Kumar, P. Maki-Arvela, O. V. Ardashov, K. P. Volcho, N. F. Salakhutdinov and D. Y. Murzin, *Materials (Basel)*, 2013, **6**, 2103-2118.
14. M. Stekrova, N. Kumar, , S. F. Díaz, P. Mäki-Arvela, & D. Y. Murzin. *Catal. Today*, 2015, 241, 237-245.
15. J. Młodzik, A. Wróblewska, E. Makuch, R. J. Wróbel, & B. Michalkiewicz. *Catal Today*, 2016, **268**, 111-120.
16. M. Groeneveld, H. L. Van Beek, W. A. Duetz, and M. W. Fraaije. *Tetrahedron*, 2016, **72**, 46 7263-7267.
17. J. H. Advani, A. S. Singh, N.H. Khan, H. C. Bajaj and A. V. Biradar, *Appl. Catal. B: Environ.*, 2020, **268**, 118456.
18. A S. Singh, J. H. Advani and A. V. Biradar, *Dalton Trans*, 2020, **49**, 7210-7217.
19. E. Vrbková, Eliška V. cilová, M. Lhotka and L. Cerven, *Catalysts*, 2020, **10**, 1244.
20. K. Ravi, D. R. Naikwadi, B. D. Bankar and A. V. Biradar, *Adv. Sustain. Syst.*, 2021, **5**, 2000212.
21. A. S. Singh, D. R. Naikwadi, K. Ravi and A. V. Biradar, *Mol Catal*, 2022, **521**,112189 .
22. R. Barakov, N. Shcherban, P.Mäki-Arvela, P. Yaremov, I. Bezverkhyy, J. Wärnä, and D. Yu. Murzin, *ACS Sustainable Chem. Eng.* 2022, 10, **20**, 6642–6656.